Quasiclassical Direct Dynamics Trajectory

Simulations of Organometallic Reactions

Daniel H. Ess*

Department of Chemistry and Biochemistry, Brigham Young University, Provo, Utah 84602

CONSPECTUS

Homogeneous metal-mediated organometallic reactions represent a very large and diverse reaction class. Density functional theory calculations are now routinely carried out and reported for analyzing organometallic mechanisms and reaction pathways. While density functional theory calculations are extremely powerful to understand the energy and structure of organometallic reactions, there are several assumptions in their use and interpretation to define reaction mechanisms and to analyze reaction selectivity. Almost always it is assumed that potential energy structures calculated with density functional theory adequately describe mechanisms and selectivity within the framework of statistical theories, for example, transition state theory and RRKM theory. However, these static structures and corresponding energy landscapes do not provide atomic motion information during reactions that could reveal nonstatistical intermediates without complete intramolecular vibrational redistribution and non-intrinsic reaction coordinate (non-IRC) pathways. While nonstatistical intermediates and non-

IRC reaction pathways are now relatively well established for organic reactions these dynamic effects have heretofore been highly underexplored in organometallic reactions. Through a series of quasiclassical density functional theory direct dynamics trajectory studies my group has recently demonstrated that dynamic effects occur in a variety of fundamental organometallic reactions, especially bond activation reactions. For example, in the C-H activation reaction between methane and [Cp*(PMe₃)Ir^{III}(CH₃)]⁺ while the density functional theory energy landscape showed a two-step oxidative cleavage and reductive coupling mechanism, trajectories revealed a mixture of this two-step mechanism and a dynamic one-step mechanism that skipped the $[Cp*(PMe_3)Ir^V(H)(CH_3)_2]^+$ intermediate. This study also showed that despite a methane σ complex being located on the density functional theory surface before oxidative cleavage and after reductive coupling this intermediate is always skipped and should not be considered an intermediate during reactive trajectories. For non-IRC reaction pathways, quasiclassical direct dynamics trajectories showed that for the isomerization of $[Tp(NO)(PMe_3)W(\eta^2-benzene)]$ to [Tp(NO)(PMe₃)W(H)(Ph)] there are many dynamic reaction pathway connections due to a relatively flat energy landscape and π coordination is not necessary for C-H bond activation through oxidative cleavage. Trajectories also showed that dynamic effects are important in selectivity for ethylene C-H activation versus π coordination in reaction with Cp(PMe₃)₂Re, and trajectories provide a more quantitative model of selectivity than transition state theory. Quasiclassical trajectories examining Au-catalyzed monoallylic diol cyclizations showed dynamic coupling of several reaction steps that include alkoxylation π bond addition, proton shuttling, and water elimination reaction steps. Overall, these studies highlight the need to use direct dynamics trajectory simulations to consider atomic motion during reactions to understand organometallic reaction mechanisms and selectivity.

KEY REFERENCES

- Carlsen, R.; Wohlgemuth, N.; Carlson, L.; Ess, D. E. Dynamical Mechanism May Avoid High-Oxidation State Ir(V)-H Intermediate and Coordination Complex in Alkane and Arene C–H Activation by Cationic Ir(III) Phosphine. *J. Am. Chem. Soc.* **2018**, *140*, 11039–11045. *Quasiclassical direct dynamics trajectories revealed that in the C-H activation reaction between methane and* [Cp*(PMe₃)Ir^{III}(CH₃)]⁺ there is both the traditional two-step oxidative cleavage/reductive coupling mechanism as well as a dynamic one-step mechanism that skips the Ir^V-H intermediate.
- Yang, B.; Schouten, A.; Ess, D. H. Direct Dynamics Trajectories Reveal Nonstatistical Coordination Intermediates and Demonstrate that σ and π-Coordination Are Not Required for Rhenium(I)-Mediated Ethylene C–H Activation. *J. Am. Chem. Soc.* 2021, 8367–8374.² Because transition-state theory did not provide a quantitatively accurate selectivity model, quasiclassical direct dynamics trajectories were used to show a nonstatistical C-H σ-coordination intermediate and direct pathways for C-H activation and π coordination.

I. INTRODUCTION

Homogeneous metal-mediated organometallic reactions range from classic elementary transformations such as oxidative addition, reductive elimination, σ -bond metathesis, migratory insertion, and oxidative coupling to more modern reactions such as β -hydrogen transfer and metal-carbene insertion. While many of these fundamental organometallic reactions have been examined with experiments, for example, kinetic isotope effects, 3,4 ultrafast spectroscopy, 5,6 and x-ray structures, the most ubiquitous direct analysis of these reactions has been with density functional theory (DFT) calculations.⁸ DFT calculations are extremely powerful to understand the energy and structure of organometallic reactions, but there are several assumptions in their use and interpretation to define reaction mechanisms and analyze reaction selectivity. One major assumption that is almost always used is that these reactions can be modeled within the context of statistical theories, such as transition state theory or RRKM theory. 9,10 Statistical theories provide a framework for translating static (i.e. potential energy only) DFT structures to reaction mechanisms and calculating and understanding reaction selectivity. In this type of statistical scenario for a two-step reaction a transition state leads to an intermediate that then leads to a product (Figure 1a). In this two-step scenario the intermediate is assumed to have atomic kinetic energy in an equilibrium distribution among harmonic vibrational modes^{11,12} and there is very fast intramolecular vibrational energy redistribution (IVR). Also, in this scenario each transition state is assumed be connected to only one minimum energy structure in the forwards and backwards reaction directions. These connections are very often based on intrinsic reaction coordinate (IRC) calculations, ¹³ which generally advance the reaction coordinate progress from the transition-state structure using the steepest descent pathway in mass-weighted coordinates without atomic velocity.

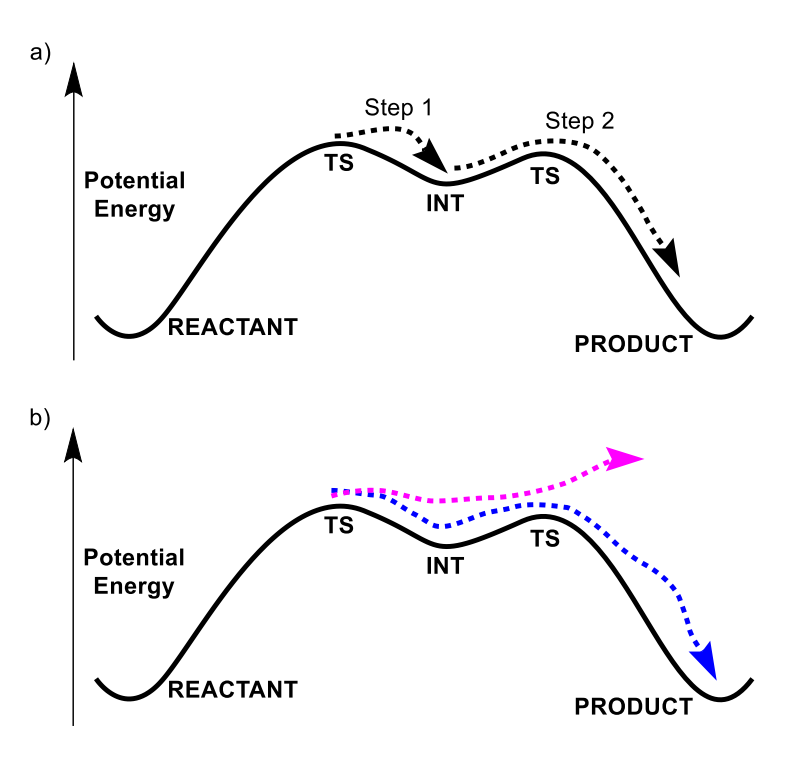


Figure 1. Qualitative potential-energy landscape (solid black line) with two steps. a) Black dotted arrows represent atomic motion of the chemical reaction along the landscape where there is complete IVR and stopping at the intermediate (INT) before crossing the second transition state (TS). b) The blue dotted arrow represents a possible nonstatistical reaction pathway where there is incomplete IVR and skipping of the intermediate. The lavender dotted line represents non-IRC motion where the reaction occurs through geometries or intermediates not part of the IRC pathway.

Over the past several years it has been my group's hypothesis that some organometallic reactions do not follow these typical statistical theory assumptions and that DFT calculated energy landscapes do not provide a complete description of reaction mechanisms and selectivity. Figure 1b illustrates possible alternative nonstatistical reaction pathways that might occur on the same potential energy surface as in Figure 1a. The blue dotted arrow represents a possible reaction pathway where there is incomplete IVR and skipping of the intermediate. The lavender dotted line represents non-IRC motion where the reaction occurs through geometries or intermediates not part of the IRC pathway. Our hypothesis is based on the rationale that during

organometallic reactions a reacting metal-ligand complex often morphs into and out of highly reactive, coordinatively unsaturated structures with high oxidative states, distorted geometries, and close spin states.

Examining the possibility that nonstatistical pathways might occur during organometallic reactions can be done with molecular dynamics trajectory simulations that provide detailed information about the timing of geometry changes and lifetime of structures during reactions. ¹⁴ While nonstatistical effects and non-IRC pathways have been explored for several organic reactions, ^{15,16,17,18} especially reactions with a potential energy surface post-transition state bifurcation, ^{19,20,21,22,23,24} these effects are only recently being identified in organometallic reactions, especially bond activation-type reactions. This account provides an overview of my group's recent quasiclassical direct dynamics simulations used to uncover nonstatistical effects and non-IRC reaction pathways in fundamental organometallic reactions. These studies have impacted the understanding of energy landscapes calculated by DFT methods and their interpretation for organometallic mechanisms and selectivity.

II. Quasiclassical direct dynamics trajectories.

Before briefly describing quasiclassical direct dynamics trajectories it is instructive to describe why IRC-based reaction pathways might be insufficient when considering organometallic reaction mechanisms and selectivity based on DFT structures. An IRC calculation is useful to identify connections on a potential energy surface through a steepest decent-type approach. Developed mainly by Fukui, ¹³ each point along the IRC pathway has no vibration, no rotation, and infinitesimal velocity. Crudely, IRCs provide an average pathway of

transforming structures. IRCs cannot generally identify nonstatistical intermediates or other effects that are the result of vibrational mode energy and kinetic energy and momentum of atoms during reactions. However, sometimes the failure of IRC calculations can hint at nonstatistical effects.

In the studies highlighted in this account, we used quasiclassical direct molecular dynamics simulations to examine the impact of atomic motion and potential energy on organometallic reaction pathways. This formulation of dynamics is inherently classical^{25,26} since the propagation of trajectory steps is performed using Newtonian equations.²⁷ In most cases we used either a Verlet integration algorithm in our Milo program²⁸ or a more sophisticated predictor-corrector algorithm that is implemented in Gaussian.^{29,30} Our Milo program is based on Singleton's Progdyn³¹ and Hase's VENUS³² programs. For most of the organometallic reactions we have examined we found nearly identical results using both algorithms.

A step size must be defined for propagation of a classical trajectory. Because the step size combined with the size of the molecular system determines the computational cost, most quasiclassical direct dynamics studies of organic reactions have used a step size in the vicinity of 1 femtosecond (fs). Unfortunately, very few studies have reported the impact of step size on trajectory results. We have found that a step size of ~0.75 fs or smaller generally provides converged organometallic trajectory results.

For direct dynamics trajectories forces are calculated at every time step during propagation, and sometimes force constants. The balance of speed and accuracy has made calculating forces with DFT methods feasible. For organometallic reactions there is a general literature consensus that M06³³ and MN15³⁴ functionals (or other similar functionals) generally

provide a balance of solid accuracy and broad treatment of different metal centers, ligands, and reaction types. However, there are still a limited number of studies that have tested the accuracy of DFT methods for organometallic reactions, especially compared to experiment. Accurate calculation of forces is critical for direct dynamics trajectories, and therefore in several of our studies we compared DFT energies with DLPNO-CCSD(T)³⁵ or CCSD(T) calculations.

The final ingredient to consider for quasiclassical dynamics simulations is the choice of generating starting trajectory configurations. In this type of dynamics simulation, a trajectory begins with the potential energy of the reacting structure as well as quantized vibrational mode energy. It can also be supplemented with rotational and translational energy. While there are different approaches for sampling vibrational modes based on a specific temperature, our studies generally used microcanonical (*NVE* ensemble) normal mode sampling where the zero-point vibrational energy level or excited vibrational energy is used based on statistical sampling, and the mode directions are randomly assigned. Trajectories are either started at a potential-energy transition-state structure with vibrationally sampled atomic velocities or started with a sampled geometry that provides a mixture of kinetic and potential energy from each vibrational mode. Starting at a transition state is advantageous because trajectory propagation can be performed chemically forwards and backwards, and this generally provides reactive trajectories.

III. One step, two steps, or something in between?

With the hypothesis that nonstatistical effects might occur in organometallic reactions that morph into and out of a high oxidative state, we used quasiclassical direct dynamics trajectories to determine the mechanism of methane C-H activation by [Cp*(PMe₃)Ir^{III}(CH₃)]⁺, ¹

which involves overall σ-bond metathesis.^{36,37} Figure 2a shows the originally considered one-step concerted and two-step reaction mechanisms. Early static (potential energy only) DFT calculations identified the mechanism and energy landscape with two steps that involves an oxidative cleavage and reductive coupling sequence with an intervening high-oxidation state Ir^V-H intermediate.³⁸ Our own evaluation of this mechanism using M06 calculations also showed two transition states and a Ir^V-H intermediate (Figure 2b).

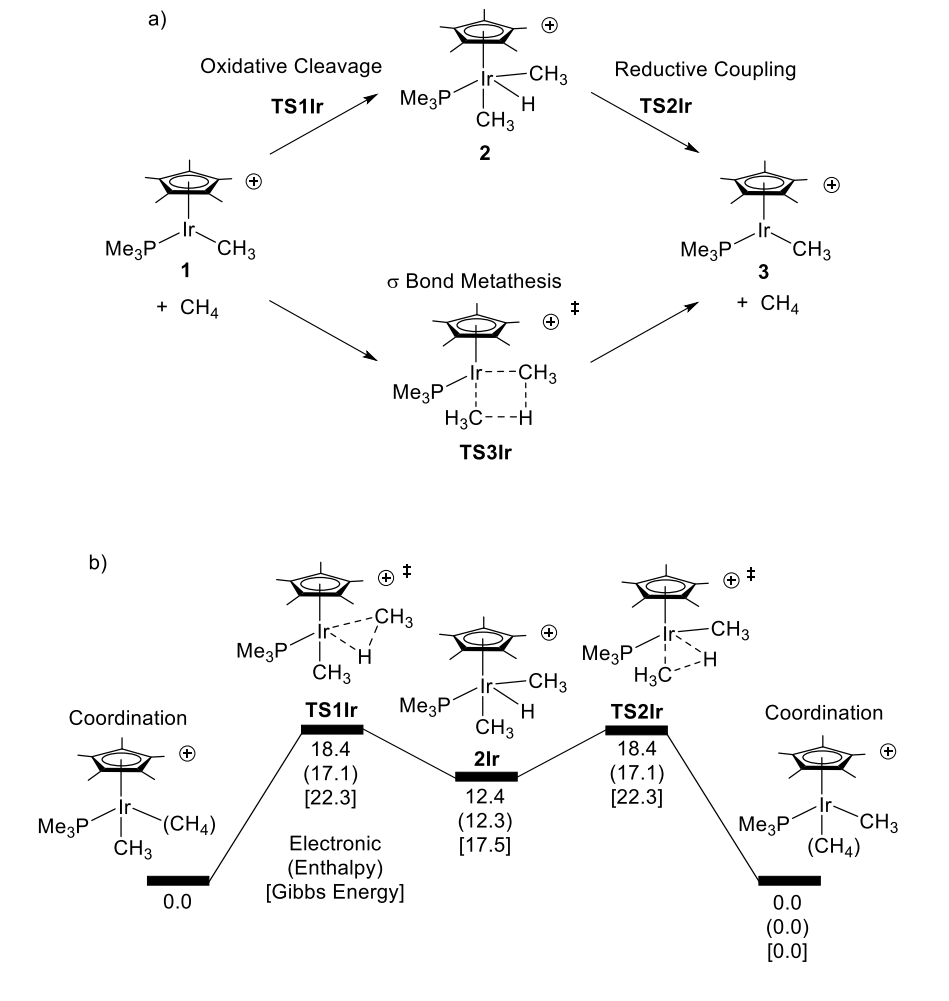


Figure 2. a) Comparison of possible oxidation cleavage/reductive coupling and σ -bond metathesis reaction pathways for methane C-H activation by $[Cp^*(PMe_3)Ir^{III}(CH_3)]^+$. b) M06 two-step potential energy landscape. Energies in kcal/mol. Reproduced with permission from ref. 1. Copyright 2018 American Chemical Society.

Using microcanonical sampling for trajectories launched from TS1Ir, in both gas-phase and implicit dichloromethane solvent, we found three major trajectory outcomes after about 1000 fs.¹ A time step of ~0.75 fs or less provided converged trajectory results and other quality DFT functionals gave similar results.³⁹ The majority outcome of trajectories displayed IVR and resulted in a persistent IrV-H structure. However, in nearly 20% of the trajectories we found nonstatistical reaction motion that skipped or bypassed the high oxidation state IrV-H structure, and this was labeled as a dynamic one-step mechanism. Figure 3a illustrates a representative example of this dynamic mechanism where the IrV-H intermediate is skipped within ~75 fs after the transition state. This dynamic mechanism is illustrated by the dotted blue arrow on the energy landscape in Figure 3b and shows the coupling of oxidative cleavage and reductive coupling steps. This dynamic merging of multiple steps is similar to the merging of multiple hydrogenation reaction steps in (Cl)(CO)(PH₃)Ru^{II}(H)(H₂)(C₂H₄) that was identified by Woo's trajectory study.⁴⁰

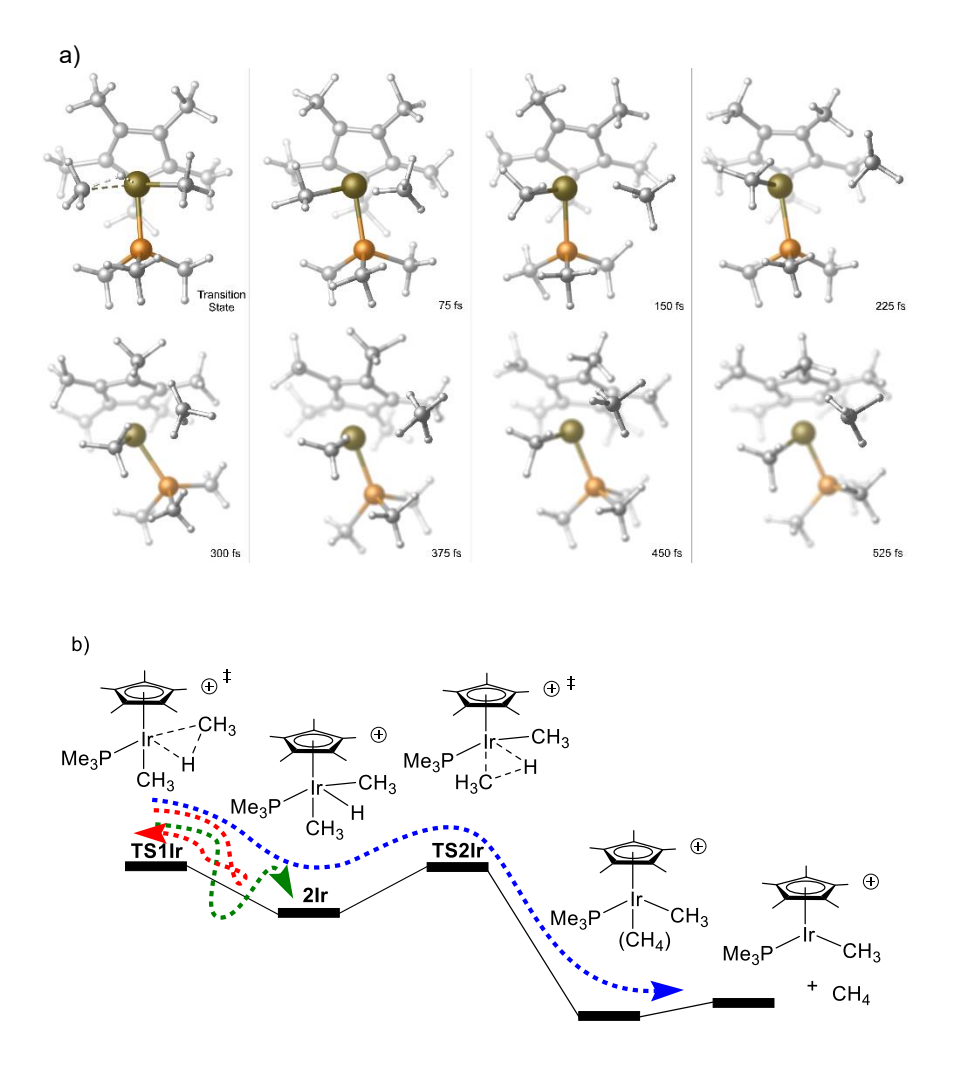


Figure 3. a) 3D images of snapshots for a representative trajectory that skips the Ir^V-H intermediate. b) Qualitative potential-energy surface overlayed with arrows representing trajectory outcomes. The green arrow represents a trajectory resulting in the Ir^V-H structure. The blue arrow represents a trajectory that bypasses the Ir^V-H structure and methane coordination complex. The red arrow represents a recrossing outcome. Reproduced with permission from ref. 1. Copyright 2018 American Chemical Society.

To visualize a representative set of trajectory outcomes for this reaction, Figure 4a plots trajectory time versus the breaking methane C-H bond length. This plot provides visual determination if the trajectory stays at the Ir^V-H intermediate or moves beyond it. This plot shows that nearly half of trajectories that bypass the Ir^V-H intermediate do so in under 500 fs from the transition state, which is on the time scale of a solvent collision and likely faster than intermolecular energy transfer, which has been estimated to be on the picosecond (ps) time scale

for organometallic reactions. 41,42,43,44 In addition to very fast dynamic skipping on the Ir-H intermediate, we also found nearly as many trajectories that skipped the intermediate after a somewhat longer time. We categorized these different trajectory scenarios as dynamically ballistic and dynamically unrelaxed mechanisms.

Another discovery from these Ir trajectories is that complete methane dissociation always occurs after reductive coupling, despite a methane coordination structure on the potential energy landscape. Trajectories also showed no methane complex prior to oxidative cleavage. This indicates that despite the mechanistic and reactive importance often placed upon C-H σ coordination complexes that this type of structure might also be skipped during reactive trajectories, especially if they are not highly stabilized. Overall, these trajectories showed that interpretation of a potential energy surface can be incomplete without consideration of dynamic atomic motion for high oxidation state endothermic intermediates that are not highly stabilized. Also, there is the possibility of multiple types of mechanisms that can occur in an organometallic reaction.

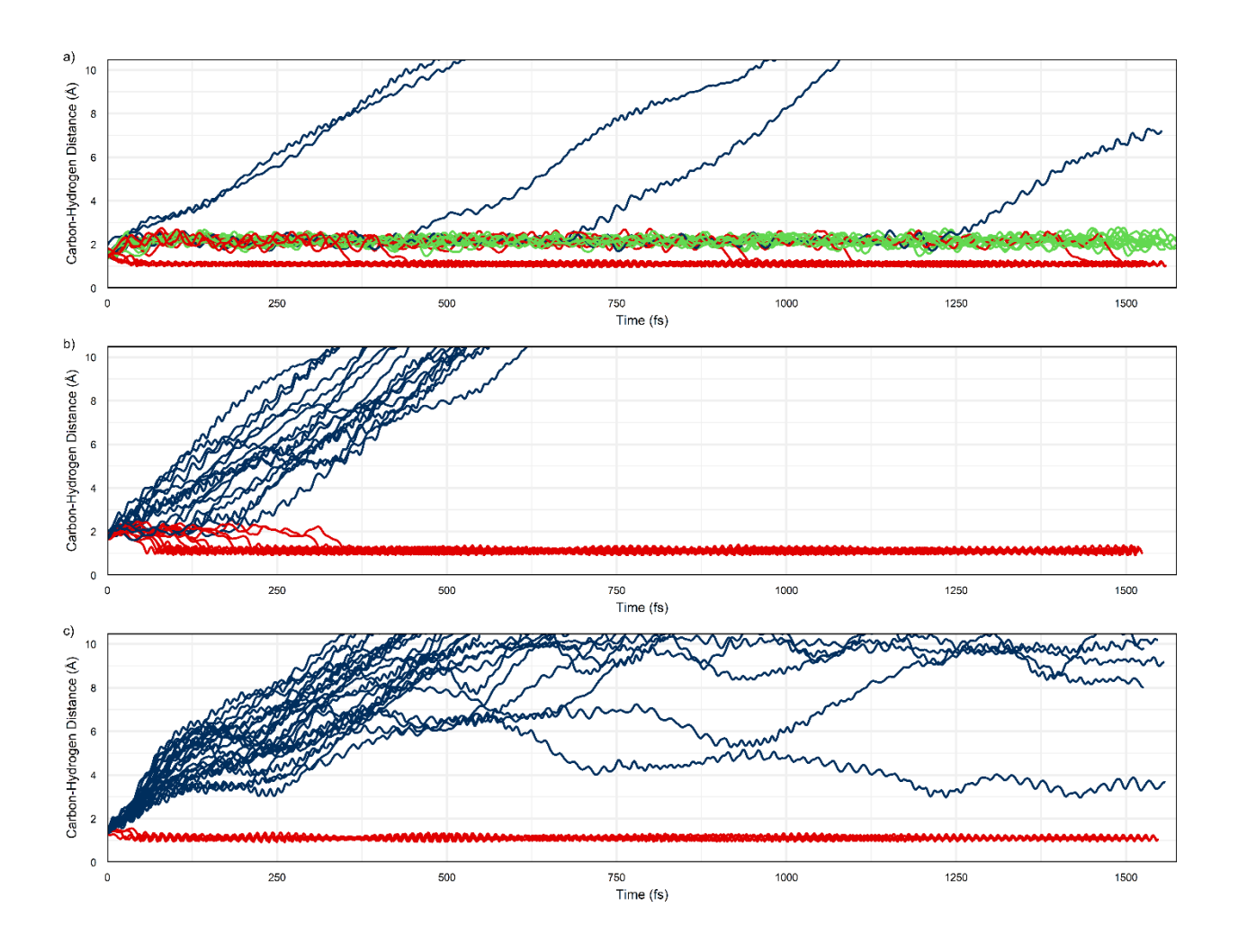


Figure 4. Plots of the breaking methane C-H bond distance (Å) versus time (fs) for 30 representative trajectories starting at the transition state. a) Ir oxidative cleavage transition state. b) Rh oxidative cleavage transition state. c) Co concerted transition state. Green lines in represent trajectories that stop at the M^V-H intermediate (two-step mechanism). Blue lines represent trajectories with long C-H distances and indicate progression beyond the M^V-H intermediate. Red lines represent recrossing. Reproduced with permission from ref. 45. Copyright 2020 American Chemical Society.

To examine the origin of the ballistic skipping of the Ir^V-H intermediate, we examined the vibrational mode excitations of every trajectory.⁴⁵ Due to the limited number of trajectories we used a statistical Fisher's exact test with a Bonferroni corrected significance level. This allowed the comparison of excitation quanta distributions between ballistic trajectories versus trajectories that ended at the Ir^V-H structure. This statistical analysis showed that ballistic

skipping had 86% of the trajectories with excitation in mode 24. Figure 5a depicts that vibrational mode 24 in **TS1Ir** (235.5 cm⁻¹) has Me-Ir-Me type bending motion that brings the transferring hydrogen from methane closer to methyl group. This suggests that the combination of mode 24 along with the reaction coordination motion likely facilitates skipping of the Ir^V-H intermediate. This type of motion coupling is related to the concept of dynamic matching that has been popularized by Carpenter for organic reactions.⁴⁶

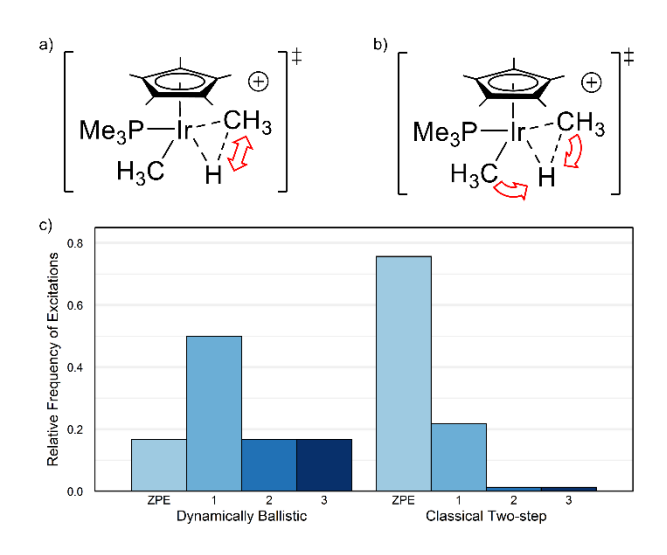


Figure 5. a) Outline of C-H bond stretching motion for the transition-state structure imaginary frequency. b) Illustration of the transition-state structure bending motion (mode 24). c) Relative frequency of excitation levels for mode 24 found in ballistic versus two-step trajectories. Reproduced with permission from ref. 45. Copyright 2020 American Chemical Society.

To consider the relationship between the potential energy landscape shape and trajectory outcomes, we examined the impact of changing the metal center from Ir to Rh and Co.⁴⁵ The Rh^V-H intermediate is less stabilized than the Ir^V-H intermediate and the Co reaction is concerted. Consistent with the energy landscape profiles providing predictive power about the relative amount of different trajectory outcomes, for Rh, despite a Rh^V-H structure located on the DFT energy landscape all trajectories skipped this intermediate between 15-200 fs after the

transition state. This indicates that the Rh reaction should be considered dynamically one step. However, the timing of the Rh reaction to progress past the Rh^V-H intermediate is slightly longer than the concerted reaction mechanism for Co where all trajectories generated the product in 15 fs after the transition state. A similar relationship between the transition metal center, energy landscape, and relative trajectory outcomes was found by Zheng for the intramolecular hydride transfer reaction resulting in metal-allyl isomerization.⁴⁷

With the discovery that reaction coordinate motion and vibrational mode excitation can lead to skipping of metal-hydride intermediates, we then examined the dynamics of the related β -hydrogen transfer mechanism that also involves this type of intermediate. We chose to focus our direct dynamics study on the β -hydrogen transfer reaction of $[Cp*Rh^{III}(Et)(ethylene)]^+$ (and Ir and Co analogs) because previous static DFT calculations showed that this Rh reaction has a two-step β -hydrogen transfer energy landscape (Figure 6).^{48,49}

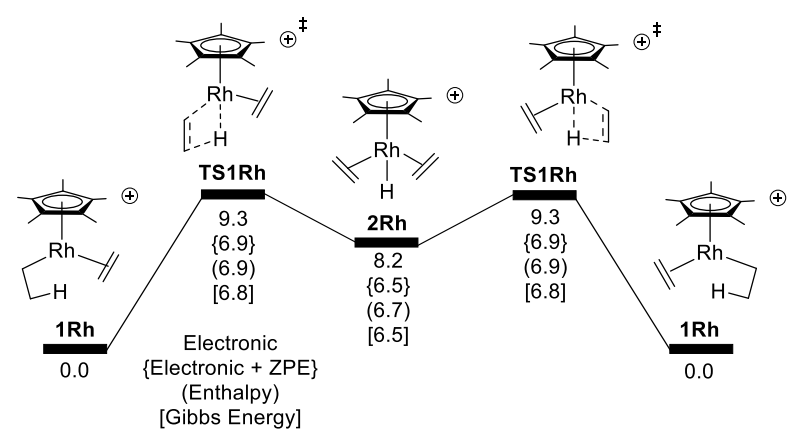


Figure 6. Potential-energy M06/6-31G**[LANL2DZ] energy landscape for β-hydrogen transfer. Energy values in kcal/mol. Reproduced with permission from ref. 50. Copyright 2020 Royal Society of Chemistry.

After confirming the two-step potential energy landscape with the M06 functional, quasiclassical trajectories commencing from the β-hydrogen transfer transition state (TS1Rh;

Figure 6) revealed complete dynamical skipping of the Rh-H intermediate. ⁵⁰ Figure 7a shows 3D depictions of time snapshots of a representative dynamically ballistic Rh trajectory. Trajectories for this β -hydrogen transfer reaction showed both ballistic unrelaxed dynamic mechanisms. In addition, because the coordination complex stays intact after β -hydrogen transfer, a third type of trajectory was also identified where the transferred hydrogen is returned to the original carbon atom in a complete reversal of the reaction, which we termed a back-and-forth trajectory (Figure 7c). Trajectories also revealed C-C bond rotation of the ethyl group after β -hydrogen transfer, which interchanges agostic interacting hydrogens.

Related to our trajectory study on the β -hydrogen transfer reaction of $[Cp*Rh^{III}(Et)(ethylene)]^+$, Chung, Wu, and Sun used dynamics trajectories to show a mixture of multistep and coupled reaction steps for hydrogen migration and boryl migration in Ru catalyzed geminal hydroboration.⁵¹ In this study they found about 25% of the trajectories showed this coupled reaction pathway while the remaining trajectories showed a two-step mechanism. Additionally, Woo reported trajectories for the concerted β -hydrogen transfer reaction of $[Cp_2Zr(Et)(ethylene)]^+$, which confirm very fast crossing of the transition state region in \sim 30-40 fs.⁵²

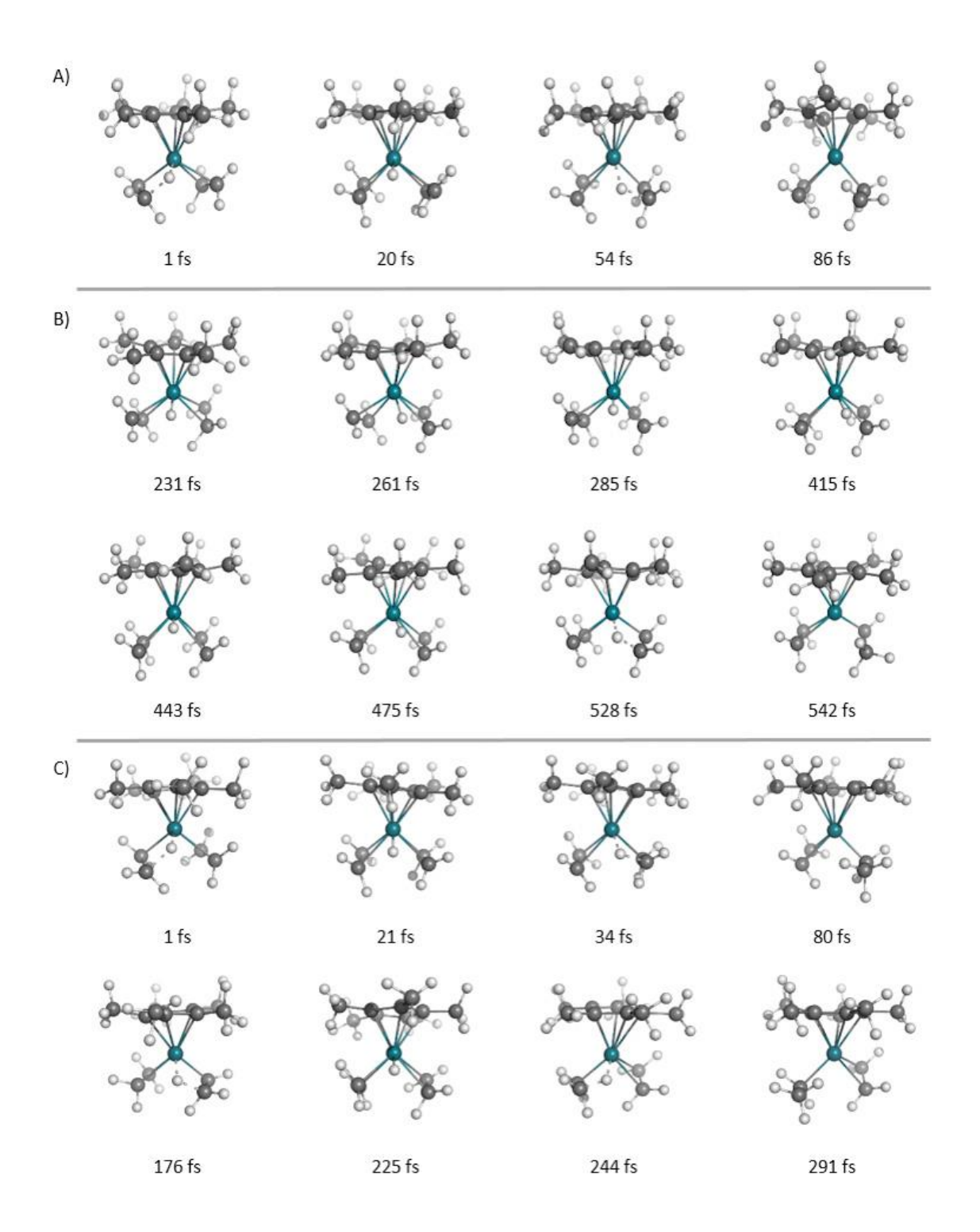


Figure 7. a) Representative dynamically ballistic trajectory. b) Representative dynamically unrelaxed trajectory. c) Representative back-and-forth trajectory. Reproduced with permission from ref. 50. Copyright 2020 Royal Society of Chemistry.

The trajectories for methane σ -bond metathesis with $[Cp*(PMe_3)Ir^{III}(CH_3)]^+$ and β -hydrogen transfer of $[Cp*Rh^{III}(Et)(ethylene)]^+$ demonstrated that dynamically coupled steps are possible in stoichiometric organometallic reactions. We wanted to identify this type of nonstatistical reaction pathway in the context of catalytic reactions. Au and Pd complexes are highly effective π -bond cyclization catalysts to construct heterocycles and are typically proposed to proceed through multistep mechanisms. Therefore, using quasiclassical trajectories we examined dynamic reaction pathways of Au phosphine catalyzed and Pd catalyzed cyclization of monoallyic diols that result in pyran products. The Au-catalyzed cyclization DFT potential energy surface landscape is outlined in Figure 8a and shows a stepwise sequence of alkoxylation π bond addition, proton shuttling, and water elimination.

Trajectories starting at the Au addition transition state (**TS1Au**) revealed that after π -addition the Au-alkyl intermediate **2Au** is always skipped or bypassed and that this transition state is dynamically coupled with both proton transfer and water elimination steps. Similar to other reactions trajectories showed both ballistic and slightly slower unrelaxed dynamic mechanisms. In contrast to Au, for Pd, due to a more stabilized metal-alkyl intermediate, only about half of the trajectories showed intermediate skipping. The other half of the trajectories showed the two-step mechanism. Figure 8b attempts to show how ballistic and unrelaxed mechanisms can short circuit catalytic cycles.

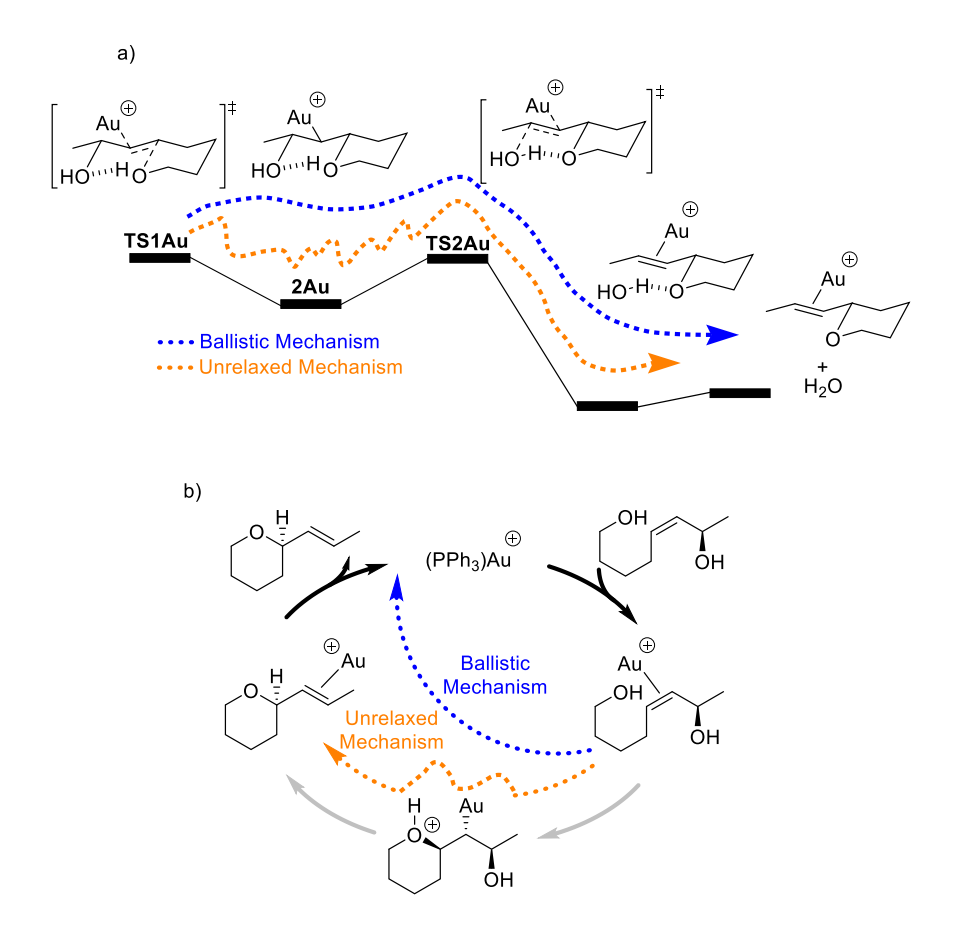


Figure 8. a) Outline of Au-catalyzed potential energy landscape showing the anti addition step followed by the anti elimination step. The dotted blue arrow outlines a ballistic reaction trajectory and the dotted orange arrow depicts an unrelaxed reaction trajectory. b) Au catalytic cycle that considers the ballistic and unrelaxed mechanisms based on trajectories. Reproduced with permission from ref. 56. Copyright 2021 American Chemical Society.

It is important to note that the dynamic coupling of reaction steps is a different nonstatistical effect than a post-transition state bifurcation where one transition state can lead to two or more products. Post-transition state bifurcations have previously been proposed for Au catalysis based on static DFT calculations.^{57,58} However, Zhang used Lagrangian-type trajectories (not quasiclassical, and akin to Car-Parrinello dynamics) to demonstrate a post-transition state bifurcation during Au-catalyzed cycloisomerization of (2-ethynylphenyl)alkynes.⁵⁹ Yu also proposed a post-transition state bifurcation for a Au-catalyzed

ring expansion/spirocyclization reaction. Recently, Wolf used DFT-based trajectories (not quasiclassical) to demonstrate that there is a bifurcation after the transition state for $(PR_3)_2Pd$ allylic halide oxidative cleavage connects to both the η^1 -allyl and η^3 -allyl structures. More akin to the skipping of an intermediate, Gutierrez recently report quasiclassical trajectories for the oxidative addition reaction step in a Ni catalyzed alkyl radical-aryl halide cross coupling reaction. Trajectories started at the Ni^{II} phenyl bromide oxidative addition transition state led to both the Ni^{III} aryl bromide intermediate as well as unrelaxed skipping leading to a Ni^{II} intermediate upon *tert*-butyl radical dissociation. 62

IV. σ-Coordination complexes.

Because reactive trajectories between [Cp*(PMe₃)Ir^{III}(CH₃)]⁺ and methane always skipped the methane σ-complex before oxidative cleavage and after reductive coupling this prompted us to examine the dynamics of proton-induced reductive elimination of (PONOP)Rh(CH₃) where a resulting [(PONOP)Rh(CH₄)]⁺ σ-complex has been experimentally detected by NMR.⁶³ Based on the DFT landscape for reductive coupling of [(PONOP)Rh(H)(CH₃)]⁺ we envisioned three possible trajectory outcomes, which are outlined with blue, black, and green dotted arrows in Figure 9.

Consistent with experiment, quasiclassical trajectories started at the reductive coupling transition state showed that most trajectories (>90%) led to the Rh-methane σ -complex (Figure 9, bottom).⁶⁴ Less than 10% of trajectories did not sample this σ -complex structure and resulted in direct methane dissociation. This indicates that the σ -complex connected to the Rh-methyl hydride is not the result of methane rebounding back to the Rh metal center due to a solvent cage

but is on the reactive trajectory pathway. However, many trajectories formed the σ -complex with paddle ball type motion where methane began to leave contact with the Rh metal but then returned to the σ -complex. This type of motion is plotted by the blue lines at the bottom of Figure 9 where there is up and down arching motion. This means that the distinction that is often made between reductive coupling and reductive elimination is blurred in this reaction. Trajectories also revealed that after reductive coupling there is very fast methane tumbling motion that generally sampled η^1 -C,H and η^2 -C,H type structures.

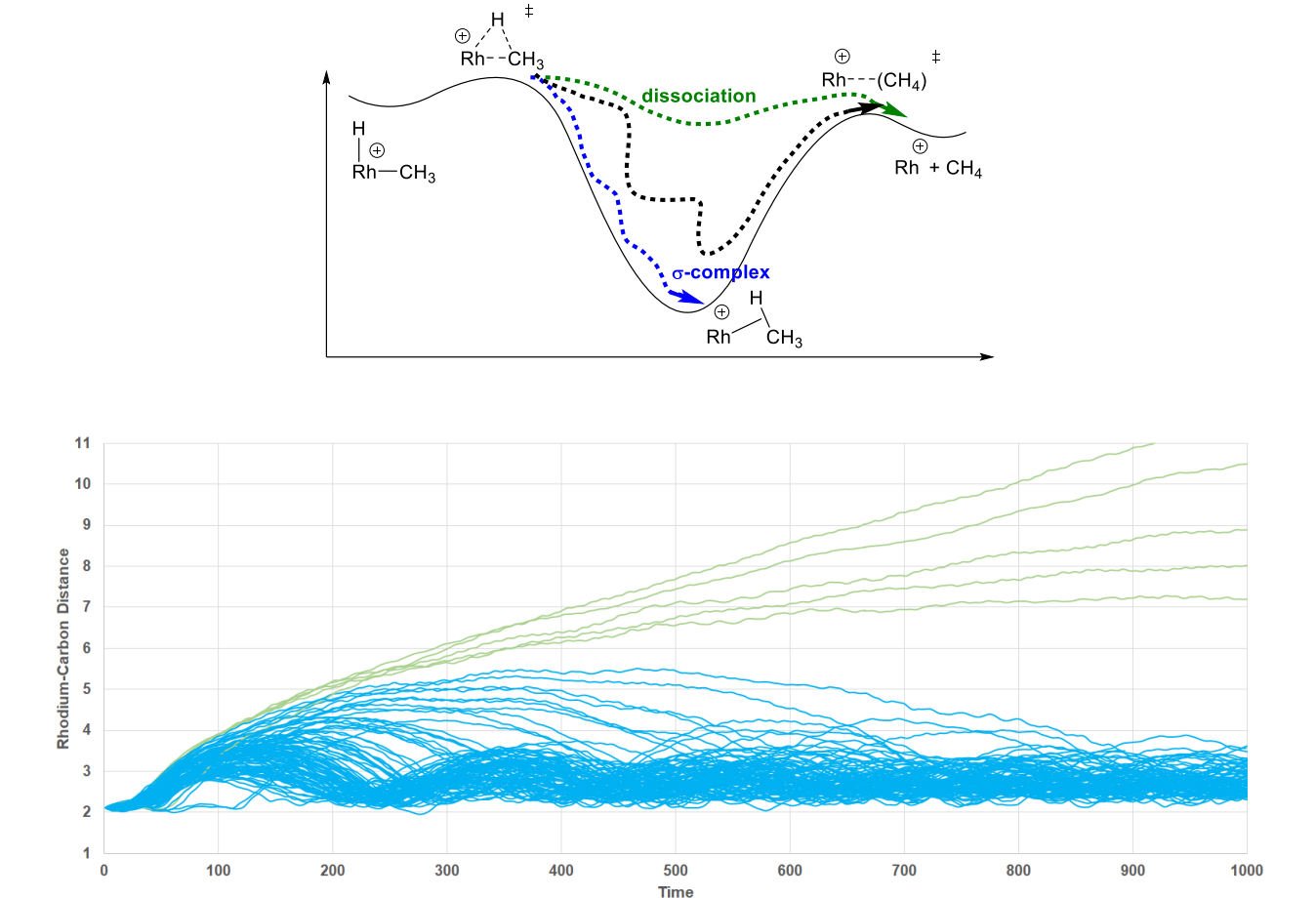


Figure 9. Top: Formation of a Rh-methane σ -complex reported by Brookhart and coworkers. Middle: Qualitative potential energy surface for reductive coupling/elimination surface showing three possible trajectory outcomes. Bottom: Plot of trajectory time (fs) versus Rh-C distance (Å). Blue lines represent trajectories leading to the Rh-methane σ -complex. Green lines represent

trajectories leading to methane dissociation. Reproduced with permission from ref. 64. Copyright 2019 American Chemical Society.

In the context of σ -bond metathesis reactions there is often a demarcation based on if a σ -complex is formed. If a complex is formed the reaction is often termed σ -complex assisted metathesis (σ -CAM).⁶⁵ If a σ -complex is not formed than the term σ -bond metathesis is applied. With the [Cp*(PMe₃)Ir^{III}(CH₃)]⁺-methane dynamically skipping the σ -complex and the [(PONOP)Rh(H)(CH₃)]⁺ reductive elimination reaction dynamically forming a σ -complex, but with paddle ball motion, we decided to use trajectories to examine the archetype σ -bond metathesis reaction of (Cp*)₂Lu(CH₃) with methane.⁶⁶ In contrast to the [(PONOP)Rh(CH₄)]⁺ σ -complex that is highly stabilized (~18 kcal/mol), the σ -complex on the potential energy surface for (Cp*)₂Lu(CH₃) σ -bond metathesis with methane is only stable by ~5 kcal/mol.

Quasiclassical trajectories for the reaction between methane and (Cp*)₂Lu(CH₃) showed this transformation to be highly concerted with extremely rapid traversing through the transition-state region and essentially no Lu-H vibration.⁶⁷ Despite a fully optimized (Cp*)₂Lu(CH₃)(CH₄) σ-complex on the potential-energy surface, this structure was never found at the end of trajectories – this intermediate was always skipped and not directly on the reaction pathway from the metathesis transition state. However, it is important to note that these are gas phase reaction trajectories (continuum solvation shows the same results) and that it is possible that with explicit consideration of solvent there would be a caging effect where methane would return to the metal center and form a σ-complex intermediate. It is unlikely that nonpolar, weakly interacting solvent would create enough friction to completely dampen methane ejection to cause trajectories to stop at the σ-complex structure.

V. Making non-IRC connections.

In addition to identifying dynamically coupled reaction steps, direct dynamics trajectories can also reveal non-IRC reaction pathways. An example where quasiclassical trajectories demonstrated multiple non-IRC reaction pathway connections was for the isomerization of $[Tp(NO)(PMe_3)W(\eta^2\text{-benzene})]$ and $[Tp(NO)(PMe_3)W(H)(Ph)]$ isomers.⁶⁸ Figure 10 shows the IRC (solid red line) pathway between the W-phenyl hydride and the $\eta^2\text{-benzene}$ coordination structure and the many non-IRC reaction pathways identified based on trajectories. While most trajectories proceeding through TS1 showed the IRC $2H\rightarrow TS1\rightarrow 2\sigma$ pathway, several trajectories showed connections between the σ -complex and the η^2 -benzene complex (2) without passing through TS2 (e.g. dark green pathway). This indicates that the weak σ -complex and surrounding vicinity provide a pathway branching area for reductive coupling/oxidative cleavage and π coordination. This branching area is likely associated with the relatively high energy set of structures associated with a weak σ -complex.

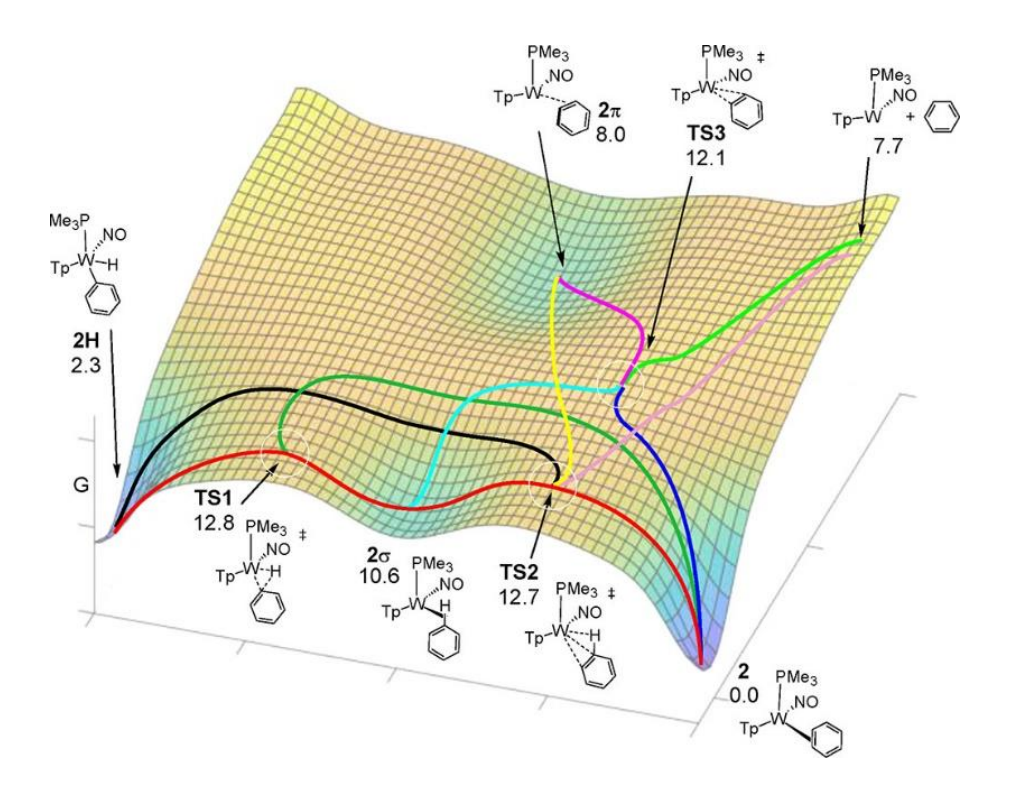


Figure 10. Multidimensional model representation to visualize reaction pathway connections based on dynamics trajectories. Energies are reported in kcal/mol. Reproduced with permission from ref. 68. Copyright 2020 American Chemical Society.

Trajectories also revealed that **TS2** is a major hub of several pathways, including connections with tightly coordinated and weakly coordinated π -complex structures. Surprisingly, many of the trajectories going through **TS2** involves the non-IRC conversion of σ -complex to the long-range π -complex rather than the tight π -complex (e.g. yellow pathway). Perhaps the most significant discovery from these trajectories is the direct connection between **2H** and benzene dissociation which indicates that η^2 -coordination is not required for insertion into the C-H bond, which is often a key mechanistic structure proposed in benzene C-H activation reactions.

Because of the discovery that η^2 -coordination is not required for C-H activation in the reaction between [Tp(NO)(PMe₃)W] and benzene, we then examined this mechanistic issue for

the reaction between Cp(PMe₃)₂Re and ethylene where η^2 -coordination was also proposed not to be necessary based on experiments.⁶⁹ The reaction of Cp(PMe₃)₂Re with ethylene results in a mixture of Re-vinyl hydride (I) to the Cp(PMe₃)₂Re(η^2 -ethylene) π -complex (II). For this Re reaction, the π -complex is more stable than the Re-vinyl hydride and therefore there is no conversion from the π -complex II to the Re-vinyl hydride I, which was taken as evidence that π -complex is not required in the mechanism for C-H activation. Figure 11 shows a potential-energy landscape and the structures located with static DFT calculations.² From an ethylene σ -coordination structure there is branching with two pathways, one pathway leading to the Revinyl hydride and the other leading to the Re(η^2 -ethylene) π -complex. While these two pathways possibly explain the reaction selectivity, CCSD(T) calculations showed that a transition-state theory approach did not match the experimental selectivity.

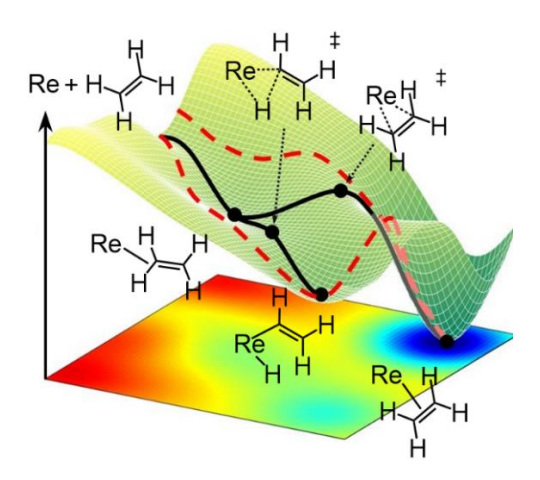


Figure 11. Qualitative 3D potential-energy landscape with black dots representing stationary points located by static DFT calculations. Solid black lines depict transition-state controlled pathways. Red dashed lines depict possible dynamic pathways. Reproduced with permission from ref. 2. Copyright 2021 American Chemical Society.

Quasiclassical direct dynamics trajectories provided a more reasonable selectivity model and revealed dynamically connected reaction pathways.² For this reaction, trajectories were

initiated at both transition-state structures as well as structures identified using metadynamics simulations. Trajectories resulted in direct formation of either the Re-vinyl hydride I or to the π -complex II. Consistent with the experimentally based proposal, trajectories leading to the Re-vinyl hydride skip or avoid both σ -coordination and π -coordination. Figure 12a shows an example trajectory where ethylene approaches the Re metal center and directly undergoes oxidative cleavage. Figure 12b shows an example trajectory where ethylene approaches the Re and forms the π -complex.

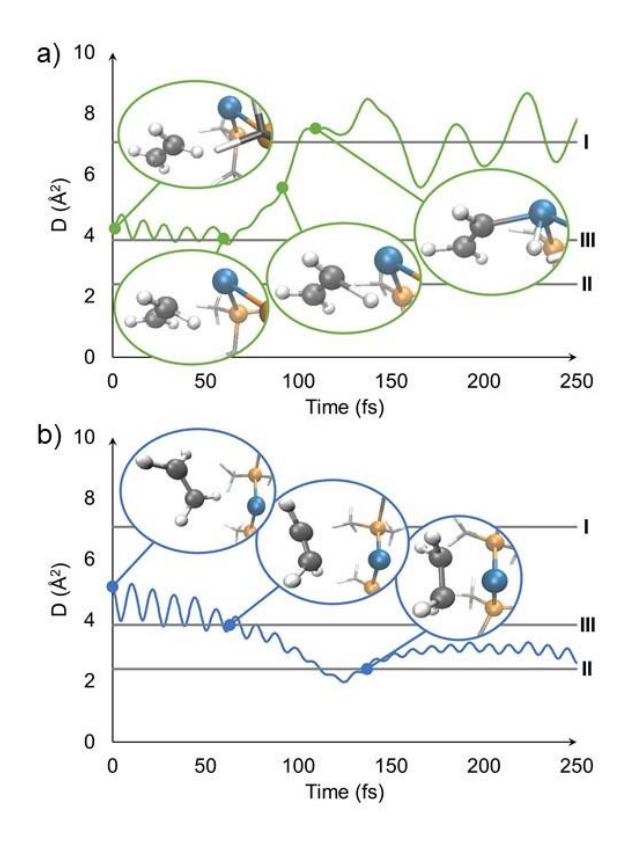


Figure 12. a) Snapshots along the way of a representative trajectory showing reaction between $Cp(PMe_3)_2Re$ and ethylene resulting in the Re-vinyl hydride **I**. b) Snapshots along the way of a representative trajectory showing reaction between $Cp(PMe_3)_2Re$ and ethylene resulting in the π-complex **II**. Reproduced with permission from ref. 2. Copyright 2021 American Chemical Society.

Trajectories also demonstrated that the C-H σ-coordination structure is a nonstatistical intermediate that does not undergo efficient IVR, which suggests that transition-state theory analysis does not provide a correct mechanism or quantitative analysis of selectivity. Related to the idea of direct insertion into an arene C-H bond and nonstatistical pathways providing a selectivity model, Díaz-Requejo, Maseras, and Pérez used trajectories to examine Cu-, Ag-, and Au-carbene C-H insertion versus Buchner ring expansion for benzene. While not quantitative due to a limited number of trajectories and model system, dynamics simulations provided significantly better correlation with experiment than transition-state theory.

As another example of organometallic reaction selectivity likely controlled by dynamic motion, we used trajectories to examine the mechanism of alkyne hydrogenation by (IMes)Ag-RuCp(CO)₂, which generates a mixture of cis and trans stilbenes.⁷¹ Figure 13 illustrates that the trajectories from the transition state for Ag-H transfer to the alkyne and provide pathways to both the trans and cis Ag-vinyl intermediates.⁷² Trajectories gave a splitting ratio at ~3:1, which was close to the experimental ratio.

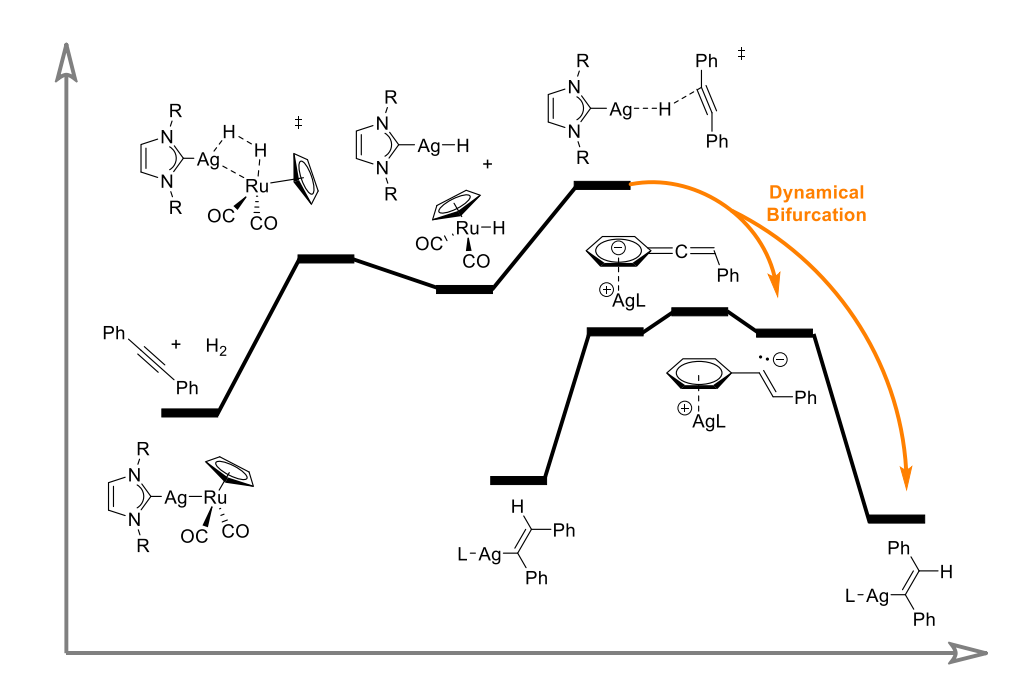


Figure 13. M06-L potential-energy landscape for H₂ semi-hydrogenation of diphenylacetylene. Adapted with permission from ref. 72. Copyright 2019 American Chemical Society.

Related to the dynamic branching found in this Ag-Ru reaction, and metal-carbene C-H insertion/Buchner ring expansion for benzene reported by Díaz-Requejo, Maseras, and Pérez, Tantillo reported trajectories highlighting a post-transition state bifurcation during the reaction Rh-carbenoid intramolecular C-H bond insertion to give β lactones.⁷³ In this reaction, trajectories revealed that in addition to the β lactone pathway there is a branching towards fragmentation generating a ketene and carbonyl. Also related to this work, trajectories have identified pathway bifurcations in Fe catalyzed Diels-Alder reactions,⁷⁴ Fe catalyzed arene amination,⁷⁵ and Pd transmetalation.⁷⁶

Conclusions

DFT calculations are routinely used to evaluate the energy and structure of organometallic reactions. In this account we highlighted that in many organometallic reactions it is necessary to go beyond static DFT calculations and consider atomic motion during reactions to understand reaction mechanisms and selectivity. Quasiclassical DFT-based direct dynamics trajectories revealed nonstatistical intermediates, dynamic coupling of multiple reaction steps, and non-IRC pathways. Examples were found in both stochiometric and catalytic organometallic reactions and are the result of a reacting metal-ligand complex that morphs into and out of highly reactive, coordinatively unsaturated structures that often have weak interaction with organic substrates. These studies revealed several general ideas, such as the shape of the energy landscape can often correlate to trajectory outcomes and that weakly coordinating intermediates

can often be skipped. Going forward it will be important to include explicit organic solvent into organometallic direct dynamics simulations similar to what Vidossich, Lledós, and Ujaque did for the (Cl)₂(H₂O)Pt^{II}(CH₄) complex in water.⁷⁷

Corresponding Author

*dhe@chem.byu.edu.

Acknowledgments

Thank you to all of the undergraduate students, graduate students, and postdocs in my lab that have made this work possible. I am especially grateful for the contributions for Ryan Carlsen, Josh Wheeler, Bo Yang, Matthew Teynor, Nathan Wohlegmuth, and Anna Schouten. This work was supported by BYU, BYU's Office of Research Computing, and the United States National Science Foundation Chemical Structure, Dynamics, and Mechanisms B (CSDM-B) Program for support under award CHE 1952420.

Biographies

Daniel H. Ess is a professor in the Department of Chemistry and Biochemistry at BYU. He received his B.S. from BYU and Ph.D. from UCLA followed by postdoctoral studies at Scripps-Florida, Caltech, and UNC Chapel Hill. His group uses and develops computational chemistry tools to discover reaction mechanisms, reactivity and selectivity principles, and design catalysts. He is the creator and director of the BYU Chem Camp program (https://chemcamp.byu.edu/).

REFERENCES

- 1. Carlsen, R.; Wohlgemuth, N.; Carlson, L.; Ess, D. E. Dynamical Mechanism May Avoid High-Oxidation State Ir(V)-H Intermediate and Coordination Complex in Alkane and Arene C– H Activation by Cationic Ir(III) Phosphine. *J. Am. Chem. Soc.* **2018**, *140*, 11039–11045.
- 2. Yang, B.; Schouten, A.; Ess, D. H. Direct Dynamics Trajectories Reveal Nonstatistical Coordination Intermediates and Demonstrate that σ and π-Coordination Are Not Required for Rhenium(I)-Mediated Ethylene C–H Activation. *J. Am. Chem. Soc.* **2021**, 8367–8374.
- 3. Jones, W. D. Isotope Effects in C–H Bond Activation Reactions by Transition Metals. *Acc. Chem. Res.* **2003**, *36*, 140–146.
- 4. Churchill, D. G.; Janak, K. E.; Wittenberg, J. S.; Parkin, G. Normal and Inverse Primary Kinetic Deuterium Isotope Effects for C–H Bond Reductive Elimination and Oxidative Addition Reactions of Molybdenocene and Tungstenocene Complexes: Evidence for Benzene σ-Complex Intermediates. *J. Am. Chem. Soc.* **2003**, *125*, 1403–1420.
- 5. Cowan, A. J.; George, M. W. Formation and Reactivity of Organometallic Alkane Complexes. *Coord. Chem. Rev.* **2008**, *252*, 2504–2511.
- 6. Asbury, J. B.; Hang, K.; Yeston, J. S.; Cordaro, J. G.; Bergman, R. G.; Lian, T. Direct Observation of a Picosecond Alkane C–H Bond Activation Reaction at Iridium. *J. Am. Chem. Soc.* **2000**, *122*, 12870–12871.
- Pike, S. D.; Thompson, A. L.; Algarra, A. G.; Apperley, D. C.; Macgregor, S. A.; Weller, A. S. Synthesis and Characterization of a Rhodium(I) σ-Alkane Complex in the Solid State. *Science* 2012, 337, 1648–1651.

- 8. Niu, S.; Hall, M. B. Theoretical Studies on Reactions of Transition-Metal Complexes. *Chem. Rev.* **2000**, *100*, 353–405.
- 9. Eyring, H. The Activated Complex in Chemical Reactions. J. Chem. Phys. 1935, 3, 107–115.
- 10. Truhlar, D. G.; Garrett, B. C.; Klippenstein, S. J. Current Status of Transition-State Theory. *J. Phys. Chem.* **1996**, *100*, 12771–12800.
- 11. Lourderaj, U.; Park, K.; Hase, W. L. Classical trajectory simulations of post-transition state dynamics. *Int. Rev. Phys. Chem.* **2009**, *113*, 2236–2253.
- 12. Spezia, R.; Martínez-Nuñez, E.; Vazquez, S.; Hase, W. L. Perspective: chemical dynamics simulations of non-statistical reaction dynamics. *Phil. Trans. R. Soc. A* **2017**, 375:20170035.
- 13. Fukui, K. The Path of Chemical Reactions The IRC Approach. *Acc. Chem. Res.* **1981**, 14, 363–368.
- 14. Paranjothy, M.; Sun, R.; Zhuang, Y.; Hase, W. L. Direct Chemical Dynamics Simulations: Coupling of Classical and Quasiclassical Trajectories with Electronic Structure Theory. *Wiley Interdiscip. Rev. Comput. Mol. Sci.* **2013**, *3*, 296–316.
- 15. Carpenter, B. K. Dynamic behavior of organic reactive intermediates. *Angew. Chem. Int. Ed.* 1998, *37*, 3340–3350.
- 16. Rehbein, J.; Carpenter, B. K. Do we fully understand what controls chemical selectivity?. *Phys. Chem. Chem. Phys.* **2011**, *13*, 20906–20922.
- 17. Carpenter, B. K. Energy Disposition in Reactive Intermediates *Chem. Rev.* **2013**, *113*, 7265–7286.
- 18. Tantillo, D. J. Recent excursions to the borderlands between the realms of concerted and stepwise: carbocation cascades in natural products biosynthesis. *J. Phys. Org. Chem.* **2008**, *21*, 561–570.

- 19. Hare, S. R.; Tantillo, D. J. Post-Transition State Bifurcations Gain Momentum Current State of the Field. *Pure Appl. Chem.* **2017**, *89*, 679–698.
- 20. Lopez, J. G.; Vayner, G.; Lourderaj, U.; Addepalli, S. V.; Kato, S.; de Jong, W. A.; Windus, T. L.; Hase, W. A. A Direct Dynamics Trajectory Study of F⁻ + CH₃OOH Reactive Collisions Reveals a Major Non-IRC Reaction Path. *J. Am. Chem. Soc.* **2007**, *129*, 9976–9985.
- 21. Doubleday, C.; Li, G.; Hase, W. L. Dynamics of the Biradical Mediating Vinylcyclopropane-Cyclopentene Rearrangement. *Phys. Chem. Chem. Phys.* **2002**, *4*, 304–312.
- 22. Bekele, T.; Christian, C. F.; Lipton, M. A.; Singleton, D. A. "Concerted" Transition State, Stepwise Mechanism. Dynamics Effects in C²-C⁶ Enyne Allene Cyclizations. *J. Am. Chem. Soc.* **2005**, *127*, 9216–9223.
- 23. Chen, Z.; Nieves-Quinones, Y.; Waas, J. R.; Singleton, D. A. Isotope Effects, Dynamic Matching, and Solvent Dynamics in a Wittig Reaction. Betaines as Bypassed Intermediates. *J. Am. Chem. Soc.* **2014**, *136*, 13122–13125.
- 24. Hare, S. R.; Li, A.; Tantillo, D. J. Post-Transition State Bifurcations Induce Dynamical Detours in Pummerer-Like Reactions. *Chem. Sci.* **2018**, *9*, 8937–8945.
- 25. Raff, L. M.; Thompson, D. L. in *Theory of Chemical Reaction Dynamics*, Ed. M. Baer (CRC, Boca Raton, FL, 1985).
- 26. Bolton, K.; Hase, W. L.; Peslherbe, G. H. in *Modern Methods for Multidimensional Dynamics Computation in Chemistry*, Ed. D. L. Thompson (World Scientific, Singapore, 1998) 143.
- 27. Helgaker, T.; Uggerud, E.; Jensen, H. J. A. Integration of the Classical Equations of Motion on ab initio Molecular-Potential Energy Surfaces Using Gradients and Hessians Application to Translational Energy-Release Upon Fragmentation. *Chem. Phys. Lett.* **1990**, *173*, 145–150.

- 28. https://github.com/DanielEss-lab/milo.
- 29. Gaussian 16, Revision B.01, Frisch, M. J.; Trucks, G. W.; Schlegel, H. B.; Scuseria, G. E.; Robb, M. A.; Cheeseman, J. R.; Scalmani, G.; Barone, V.; Petersson, G. A.; Nakatsuji, H.; Li, X.; Caricato, M.; Marenich, A. V.; Bloino, J.; Janesko, B. G.; Gomperts, R.; Mennucci, B.; Hratchian, H. P.; Ortiz, J. V.; Izmaylov, A. F.; Sonnenberg, J. L.; Williams-Young, D.; Ding, F.; Lipparini, F.; Egidi, F.; Goings, J.; Peng, B.; Petrone, A.; Henderson, T.; Ranasinghe, D.; Zakrzewski, V. G.; Gao, J.; Rega, N.; Zheng, G.; Liang, W.; Hada, M.; Ehara, M.; Toyota, K.; Fukuda, R.; Hasegawa, J.; Ishida, M.; Nakajima, T.; Honda, Y.; Kitao, O.; Nakai, H.; Vreven, T.; Throssell, K.; Montgomery, J. A., Jr.; Peralta, J. E.; Ogliaro, F.; Bearpark, M. J.; Heyd, J. J.; Brothers, E. N.; Kudin, K. N.; Staroverov, V. N.; Keith, T. A.; Kobayashi, R.; Normand, J.; Raghavachari, K.; Rendell, A. P.; Burant, J. C.; Iyengar, S. S.; Tomasi, J.; Cossi, M.; Millam, J. M.; Klene, M.; Adamo, C.; Cammi, R.; Ochterski, J. W.; Martin, R. L.; Morokuma, K.; Farkas, O.; Foresman, J. B.; Fox, D. J. Gaussian, Inc., Wallingford CT, 2016.
- 30. Millam, J. M.; Bakken, V.; Chen, W.; Hase, W. L.; Schlegel, H. B. Ab initio classical trajectories on the Born-Oppenheimer Surface: Hessian-Based Integrators using Fifth Order Polynomial and Rational Function Fits. *J. Chem. Phys.* **1999**, *111* 3800–3805.
- 31. Singleton, D. A.; Hang, C.; Szymanski M. J.; Greenwald, E. E. A New Form of Kinetic Isotope Effect. Dynamic Effects on Isotopic Selectivity and Regioselectivity. *J. Am. Chem. Soc.*, **2003**, *125*, 1176–1177.
- 32. Hase, W. L.; Duchovic, R. J.; Hu, X.; Komornicki, A.; Lim, K. F.; Lu, D.-H.; Peslherbe, G. H.; Swamy, K. N.; Linde, S. R. V.; Varandas, A.; Wang, H.; Wolfe, R. J. VENUS96: A General Chemical Dynamics Computer Program. *QCPE*, **1996**, *16*, 671.

- 33. Zhao, Y.; Truhlar, D. G. The M06 Suite of Density Functionals for Main Group Thermochemistry, Thermochemical Kinetics, Noncovalent Interactions, Excited States, and Transition Elements: Two New Functionals and Systematic Testing of Four M06-Class Functionals and 12 Other Functionals. *Theor. Chem. Acc.* **2008**, *120*, 215–241.
- 34. Yu, H. S.; He, X.; Li, S. L.; Truhlar, D. G. MN15: A Kohn-Sham Global-Hybrid Exchange-Correlation Density Functional with Broad Accuracy for Multi-Reference and Single-Reference Systems and Noncovalent Interactions. *Chem. Sci.* **2016**, *7*, 5032–5051.
- 35. Demel, O.; Pittner, J.; Neese, F. A Local Pair Natural Orbital-Based Multireference Mukherjee's Coupled Cluster Method. *J. Chem. Theory Comput.* **2015**, *11*, 3104–3114.
- 36. Burger, P.; Bergman, R. G. Facile intermolecular activation of carbon-hydrogen bonds in methane and other hydrocarbons and silicon-hydrogen bonds in silanes with the iridium(III) complex Cp*(PMe₃)Ir(CH₃)(OTf). *J. Am. Chem. Soc.* **1993**, *115*, 10462–10463.
- 37. Arndtsen, B. A.; Bergman, R. G. Unusually mild and selective hydrocarbon CH bond activation with positively charged iridium (III) complexes. *Science* **1995**, *115*, 1970–1973.
- 38. Strout, D. L.; Zarić, S.; Niu, S.; Hall, M. B. Methane metathesis at a cationic iridium center. J. Am. Chem. Soc. 1996, 118, 6068–6069.
- 39. Carlsen, R.; Jenkins, J. R.; Ess, D. H. Molecular Dynamics Analysis of the Cationic Cp*(PMe₃)Ir(CH₃) Methane C-H Activation Mechanism. *Faraday Discussions*, **2019**, *220*, 414-424
- 40. Rowley, C. N.; Woo, T. K. A Path Sampling Study of Ru-Hydride-Catalyzed H₂ Hydrogenation of Ethylene. *J. Am. Chem. Soc.* **2008**, *130*, 7218–7219.

- 41. Mizutani, Y.; Kitagawa, T. Vibrational Energy Relaxation of Metalloporphyrins in a Condensed Phase Probed by Time-Resolved Resonance Raman Spectroscopy. *Bull. Chem. Soc. Jpn.* **2002**, *75*, 623–639.
- 42. Eckert, P. A.; Kubarych, K. J. Oxidation-State-Dependent Vibrational Dynamics Probed with 2D-IR. *J. Phys. Chem. A* **2017**, *121*, 2896–2902.
- 43. Owrutsky, J. C.; Raftery, D.; Hochstrasser, R. M. Vibrational relaxation dynamics in solutions. *Annu. Rev. Phys. Chem.* **1994**, *45*, 519-555.
- 44. Li, Z.; Sansom, R.; Bonella, S.; Coker, D. F.; Mullin, A. S. Trajectory study of supercollision relaxation in highly vibrationally excited pyrazine and CO₂. *J. Phys. Chem. A* **2005**, *109*, 7657–7666.
- 45. Teynor, M. S.; Carlsen, R.; Ess, D. H. Relationship Between Energy Landscape Shape and Dynamics Trajectory Outcomes for Methane C-H Activation by Cationic Cp*(PMe₃)Ir/Rh/Co(CH₃). *Organometallics*, **2020**, *39*, 1393–1403.
- 46. Carpenter, B. K. Dynamic Matching: The Cause of Inversion of Configuration in the [1,3] Sigmatropic Migration?. *J. Am. Chem. Soc.* **1995**, *117*, 6336–6344.
- 47. Zheng, C. Divergent Pathways and Dynamic Effects of Intramolecular Hydride Transfer Reactions Mediated by Cp*M(III) Complexes (M = Co, rh, Ir). *Cin. J. Chem.* **2020**, *38*, 1579–1584.
- 48. Brookhart, M.; Lincoln, D. M.; Bennett, M. A.; Pelling, S. Dynamics of Agostic Complexes of the Type C₅R₅(C₂H₄)M(CH₂CH₂-μ-H)+. Energy Differences between and Ancillary Ligand Control of Agostic and Terminal Hydride Structures. J. *Am. Chem. Soc.* **1990**, *112*, 2691–2694.

- 49. E. Fooladi, A. Krapp, O. Sekiguchi, M. Tilset, E. Uggerud, Mechanism for C–H bond activation in ethylene in the gas phase *vs.* in solution vinylic or agostic? Revisiting the case of protonated Cp*Rh(C₂H₄)₂. *Dalton Trans.* **2010**, *39*, 6317–6326.
- 50. Wheeler, J.; Carlsen, R.; Ess, D. H. Mechanistic Molecular Motion of Transition-Metal Mediated β-Hydrogen Transfer: Quasiclassical Trajectories Reveal Dynamically Ballistic, Dynamically Unrelaxed, Two Step, and Concerted Mechanisms. *Dalton Trans.* **2020**, *49*, 7747–7757.
- 51. Feng, Q.; Wu, H.; Li, X.; Song, L.; Ghung, L. W.; Wu, Y-D.; Sun, J. Ru-Catalyzed Geminal Hydroboration of Silyl Alkynes via a New gem-Addition Mechanism. *J. Am. Chem. Soc.* **2020**, *142*, 13867–13877.
- 52. Rowley, C. N.; Woo, T. K. Reaction Dynamics of β-Hydrogen Transfer in the Zirconocene Olefin Polymerization Catalyst: A DFT Path Sampling Study. *Organometallics* **2008**, *27*, 6405-6407.
- 53. Aponick, A.; Li, C.-Y.; Biannic, B. A. Au-catalyzed cyclization of monoallylic diols. *Org. Lett.* **2008**, *10*, 669–671.
- 54. Kawai, N.; Lagrange, J.-M.; Ohmi, M.; Uenishi, J. Palladium-catalyzed stereospecific synthesis of 2,6-disubstituted tetrahydropyrans: 1,3-chirality transfer by an intramolecular oxypalladation reaction. *J. Org. Chem.* **2006**, *71*, 4530–4537.
- 55. Ghebreghiorgis, T.; Biannic, B.; Kirk, B. H.; Ess, D. H.; Aponick, A. The importance of hydrogen bonding to stereoselectivity and catalyst turnover in gold-catalyzed cyclization of monoallylic diols. *J. Am. Chem. Soc.* **2012**, *134*, 16307–16318.

- 56. Teynor, M. S.; Scott, W.; Ess, D. H. Catalysis with a Skip: Dynamically Coupled Addition, Proton Transfer, and Elimination during Au- and Pd-Catalyzed Diol Cyclizations. *ACS Catal.* **2021**, *11*, 10179–10189.
- 57. Noey, E. L.; Wang, X.; Houk, K. N. Selective Gold(I)-Catalyzed Formation of Tetracyclic Indolines: A Single Transition Structure and Bifurcations Lead to Multiple Products. *J. Org. Chem.* **2011**, *76*, 3477–3483.
- 58. Zhang, L.; Wang, Y.; Yao, Z-J.; Wang, X.; Yu, Z-X. Kinetic or Dynamic Control on a Bifurcating Potential Energy Surface? An Experimental and DFT Study of Gold-Catalyzed Ring Expansion and Spirocyclization of 2-Propargyl-β-tetrahydrocarbolines. *J. Am. Chem. Soc.* **2015**, *137*, 13290–13300.
- 59. Ye, L.; Wang, Y.; Aue, G. H.; Zhang, L. Experimental and Computational Evidence for Gold Vinylidenes: Generation from Terminal Alkynes via a Bifurcation Pathway and Facile C-H Insertions. *J. Am. Chem. Soc.* **2012**, *134*, 31–34.
- 60. Zhang, L.; Wang, Y.; Yao, Z-J.; Wang, X.; Yu, Z-X. Kinetic or Dynamic Control on a Bifurcating Potential Energy Surface? An Experimental and DFT Study of Gold-Catalyzed Ring Expansion and Spirocyclization of 2-Propargyl-β-tetrahydrocarbolines. *J. Am. Chem. Soc.* **2015**, *137*, 13290–13300.
- 61. Kpante, M.; Wolf, L. M. Pathway Bifurcations in the Activation of Allylic Halides by Palladium and Their Influence on the Dynamics of η^1 and η^3 Allyl Intermediates. *J. Org. Chem.* **2021**, *86*, 9637-9650.
- 62. Yuan, M.; Song, Z.; Badir, S. O.; Molander, G. A.; Gutierrez, O. On the Nature of C(sp³)—C(sp²) Bond Formation in Nickel-Catalyzed Tertiary Radical Cross-Couplings: A Case Study of

Ni/Photoredox Catalytic Cross-Coupling of Alkyl Radicals and Aryl Halides. *J. Am. Chem. Soc.* **2020**, *142*, 7225–7234.

- 63. Bernskoetter, W. H.; Schauer, C. K.; Goldberg, K. I.; Brookhart, M. Characterization of a Rhodium(I) σ-Methane Complex in Solution. *Science* **2009**, *326*, 553–556.
- 64. Carlsen, R.; Jenkins, J. R.; Chuang, J.; Pugh, S. L.; Ess, D. H. Paddle Ball Dynamics During Rh-Methyl to Rh-Methane σ-Complex Reductive Elimination. *Organometallics* **2019**, *38*, 2280–2287.
- 65. Perutz, R. N.; Sabo-Etienne, S. The σ -CAM mechanism: σ complexes as the basis of σ -bond metathesis at late-transition-metal centers. *Ang. Chem. Int. Ed.* **2007**, *46*, 2578–2592.
- 66. Watson, P. L. Methane exchange reactions of lanthanide and early-transition-metal methyl complexes. *J. Am. Chem. Soc.* **1983**, *105*, 6491–6493.
- 67. Carlsen, R.; Maley, S. M.; Ess, D. H. Timing and Structures of σ-Bond Metathesis C–H Activation Reactions from Quasiclassical Direct Dynamics Simulations. *Organometallics*, **2021**, 40, 1454–1465.
- 68. Smith, J. A.; Schouten, A.; Wilde, J. H.; Westendorff, K. S.; Dickie, D. A.; Ess, D. H.; Harmen, W. D. Experiments and Direct Dynamics Simulations Reveal a Network of Reaction Pathways for Tungsten η^2 -Arene Aryl Hydride Equilibria. *J. Am. Chem. Soc.* **2020**, *142*, 16437–16454.
- 69. Wenzel, T. T.; Bergman, R. G. Inter- and Intramolecular Insertion of Rhenium into Carbon-Hydrogen Bonds. *J. Am. Chem. Soc.* **1986**, *108*, 4856–4867.

- 70. Fructos, M. R.; Besora, M.; Braga, A. A. C.; Díaz-Requejo, Maseras, F.; Pérez, P. J. Mechanistic studies on gold-catalyzed direct arene C–H bond functionalization by carbene insertion: the coinage-metal effect. *Organometallics* **2017**, *36*, 172–179.
- 71. Karunananda, M. K.; Mankad, N. P. *E*-Selective Semi-Hydrogenation of Alkynes by Heterobimetallic Catalysis. *J. Am. Chem. Soc.* **2015**, *137*, 14598–14601.
- 72. Zhang, Y.; Karunananda, M.; Williams, W.; Clark, K.; Mankad, N.; Ess, D. H. Dynamically Bifurcating Hydride Transfer Mechanism and Origin of Inverse Kinetic Isotope Effect for Heterodinuclear AgRu-Catalyzed Alkyne Semi-Hydrogenation. *ACS Catal.* **2019**, *9*, 2657–2663.
- 73. Hare, S. R.; Tantillo, D. J. Cryptic post-transition state bifurcations that reduce the efficiency of lactone-forming Rh-carbenoid C–H insertions. *Chem. Sci.*, **2017**, *8*, 1442–1449.
- 74. Unusual KIE and dynamics effects in the Fe-catalyzed hetero-Diels-Alder reaction of unactivated aldehydes and dienes. Yang, Y.; Zhang, X. Zhong, L-P.; Lan, J.; Li, C-C.; Chung, L. W. *Nat. Commun.* **2020**, *11*, 1850.
- 75. Li, B.; Li, Y.; Dang, Y.; Houk, K. N. Post-Transition State Bifurcation in Iron-Catalyzed Arene Aminations. *ACS Catal.* **2021**, *11*, 6816–6824.
- 76. Pu, M.; Sanhueza, I. A.; Senol, E.; Schoenebeck, F. Divergent Reactivity of Stannane and Silane in the Trifluoromethylation of Pd^{II}: Cyclic Transition State versus Difluorocarbene Release. *Angew. Chem. Int. Ed.* **2018**, *57*, 15081–15085.
- 77. Vidossich, P.; Ujaque, G.; Lledós, A. Pt^{II} as a proton shuttle during C–H bond activation in the Shilov process. *Chem. Commun.* **2012**, *48*, 1979–1981.

